Dynamic Behaviour of Tetramethylethylene Diamine (TMEDA) Ligands in Solid Organolithium Compounds: A Variable Temperature ^{13}C and ^{15}N CP/MAS NMR Study

Wolfgang Baumann, Yuri Oprunenko and Harald Günther *

Universität Siegen, Fachbereich 8, OCII, D-57068 Siegen

Z. Naturforsch. **50a**, 429–438 (1995); received November 8, 1994

Dedicated to Professor Dr. W. Müller-Warmuth on the occasion of his 65th birthday

The dynamic behaviour of tetramethylethylene diamine (TMEDA) ligands in three organometallic complexes, dimeric phenyllithium, [Li(tmeda)μ-Ph]$_2$ (**1**), lithium cyclopentadienide, [Li(tmeda)]C_5H_5 (**2**), and dilithium naphthalendiide, *trans*-[Li(tmeda)]$_2C_{10}H_8$ (**3**), has been studied by CP/MAS ^{13}C and ^{15}N as well as ^7Li MAS NMR spectroscopy of powdered samples. Two dynamic processes with free activation enthalpies of 40 and 68 kJ mol^{-1}, respectively, were detected for **1**. The first one can be assigned to ring inversion of the five-membered Li-TMEDA rings, while the second is caused by a complete rotation of the TMEDA ligands or a ring inversion of the central four-membered C–Li–C–Li metallacycle. Fast rotation of the ligands on the NMR time scale was found for **2**, while **3** shows 180° ring flips of the Li-TMEDA groups, which are characterized by an energy barrier $\Delta G^{\neq}$ (317) of 64 kJ mol^{-1}.

Key words: CP/MAS NMR, ^{13}C-NMR, ^{15}N-NMR, ^7Li NMR, dynamic processes, organometallics.

Introduction

Alkali metal organic compounds are characterized by aggregation and extensive coordination with ethereal solvent molecules or donor ligands like di- and triamines [1]. In solution, the resulting aggregates are dynamic and *intra-* as well as *inter*-aggregate exchange processes take place [2]. In addition, quite a number of ligands may show internal rotation or ring inversion [3], and during such processes coordinative bonds between the donor atoms and the alkali metal may be broken and reformed [4]. This type of dynamic behaviour is thus also important with respect to the reactivity of these systems, and quantitative data for *intra*-aggregate dynamics as well as for bond breaking and bond forming processes are of general interest.

In the solid, *inter*-aggregate exchange is absent, however there is considerable evidence for *intra*-aggregate dynamic behaviour even in crystalline compounds [5–8]. In many of the X-ray investigations of such systems large thermal anisotropy parameters were found, e.g. for the nitrogen and for the methylene carbon atoms of diamine ligands [1 d, 9]. This points to high mobility of these moieties also in the solid phase. It is a unique feature of NMR spectroscopy that such dynamic processes can be traced in solids by CP/MAS NMR experiments via lineshape changes [10, 11], dipolar broadening [12], two-dimensional exchange spectroscopy [13, 14], or $T_{1\varrho}$ measurements [15]. In the present communication we report NMR results relevant for the dynamic behaviour in three organolithium compounds, where the dynamic processes involve in all cases the diamine ligand N,N,N′N′-tetramethylethylenediamine (TMEDA). Specifically we have studied dimeric phenyllithium, [Li(tmeda)μ-Ph]$_2$ (**1**), a system with lithium-carbon σ-bonds, and two polyhapto-bound systems, lithiumcyclopentadienide, [Li(tmeda)]C_5H_5 (**2**), and dilithiumnaphthalenediide, *trans*-[Li(tmeda)]$_2C_{10}H_8$ (**3**), with π-bound lithium. X-ray structures, which are important for the interpretation of the NMR results are available for **1** [6] and for **3** [5] as for trimethylsilyl derivatives of **2** [7, 8].

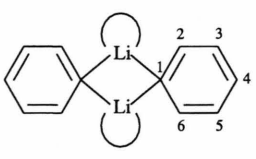

1

2

Reprint requests to: Prof. Dr. H. Günther.

0932-0784 / 95 / 0400-0429 $ 06.00 © – Verlag der Zeitschrift für Naturforschung, D-72027 Tübingen

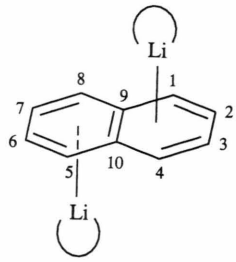

3

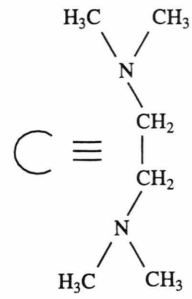

Results and Discussion

1. Phenyllithium Dimer [Li(tmeda)μ-Ph]$_2$ (1)

The dimer **1** has already been investigated by solid state NMR, however, at lower field strength and resolution and without studying dynamic phenomena [16]. The ^{13}C chemical shifts were found to resemble closely those measured in solution. Later, a ^{7}Li NMR study has appeared where the quadrupolar coupling constants of lithium in various phenyllithium aggregates were reported [17].

Our measurements were performed at 75.5 MHz for ^{13}C, 30.4 MHz for ^{15}N, and 116.6 MHz for ^{7}Li. Already at room temperature the ^{13}C CP/MAS NMR spectrum of **1** (Fig. 1) clearly indicates *intra*-aggregate mobility: the methylene carbons of the TMEDA ligands yield a strongly broadened signal (half width approx. 600 Hz) at 57 ppm, while the remaining carbon resonances have linewidths around 100 Hz. Temperature variation results in different lineshapes. A spectrum which is compatible with the solid state structure as determined by an X-ray investigation [6] (see below) is recorded at 190 K. Here, all expected ^{13}C resonances are detected, and the low symmetry of the complex (C_2) is reflected in the non-equivalences found for the aromatic carbon resonances as well as for those those of the TMEDA ligand. The ^{13}C chemical shifts measured at this temperature are collected in Table 1, which also contains the solution data.

Further evidence for dynamic processes is obtained from the ^{15}N CP/MAS spectrum of **1**. At room temperature (RT) it shows two lines, separated by 1.5 ppm (Table 2), which coalesce at 326 K to a single resonance (Figure 2).

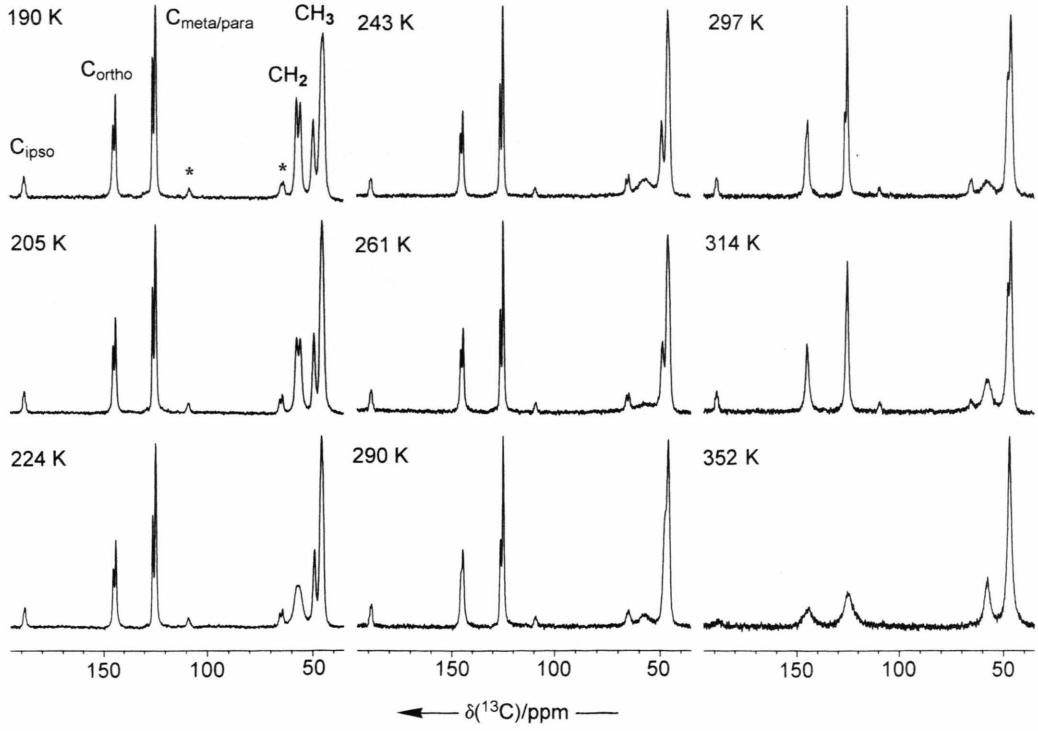

Fig. 1. 75.47 MHz ^{13}C CP/MAS NMR spectrum of [Li(tmeda)μ-Ph]$_2$ (**1**) at different temperatures; spinning speed 6 kHz; rotational side bands are marked (*).

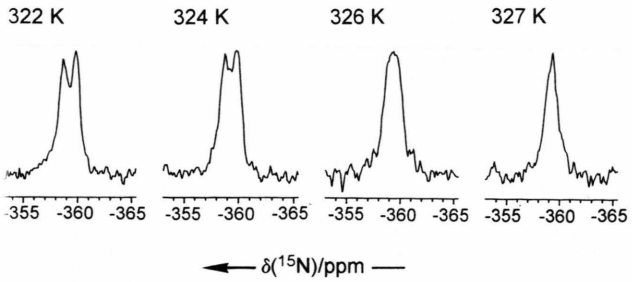

Fig. 2. 30.42 MHz ^{15}N CP/MAS NMR spectrum of **1** at different temperatures; spinning speed 2.5 kHz.

Table 1. Solid state ^{13}C NMR data[a] (ppm) for **1**–**3** (solution data in parenthesis).

	C-1	C-2,6	C-3,5	C-4	CH_2	CH_3	T(K)
1	188.1	144.9	125.6		57.3	49.3	190
		143.7	124.2		55.5	44.7	
	(187.3	144.9	124.9	123.4	56.9	46.3	173)[b]
2	104.0	–	–	–	56.5	46.7	343
	(102.8[c]				56.2[d]	46.1[d]	RT)
	C-1,4	C-2,3	C-9,10				
3	81.3	112.6	164.0		57.1	44.4	297
	84.5	115.1				45.5	
						48.2	
						48.8	
	(82.1	113.2	163.7		58.5	46.6	293)[e]

[a] Indirectly referenced to ext. tetramethylsilane;
[b] [18];
[c] [19];
[d] Data for the 1,3-di-t.butyl compound from [20];
[e] [21].

1	**2**	**3**
−358.2	−360.3	−357.9
−359.7		−360.8

Table 2. Solid state ^{15}N NMR[a] data for **1**–**3** at 290 K.

[a] Indirectly referenced to ext. nitromethane.

Apart from these lineshape changes, indirect evidence for *intra*-aggregate dynamics comes from two other observations. Firstly, a ^{13}C CP/MAS experiment with non-quaternary carbon suppression (NQS experiment [22]) indicates that at a temperature above 310 K the dipolar couplings are strongly reduced. Here, the signal of the methylene carbons is clearly observed with practically unperturbed intensity even after a dephasing delay of 40 μs. Secondly, the sideband pattern oberved in the ^{7}Li MAS NMR spectrum of **1** is temperature-dependent. As Fig. 3a shows, the quadrupolar ^{7}Li nucleus with a spin quantum number $I = 3/2$ yields, aside from the central line for the $1/2 \rightarrow -1/2$ transition at 3.6 ppm rel. to LiBr (halfwidth ca. 400 Hz), a number of spinning sidebands [23]. The extent of the sideband pattern is a measure of the quadrupolar interaction and reflects the magnitude of the electric field gradient at the nucleus and the asymmetry of the chemical environment, that is, the coordination sphere. *Intra*-molecular dynamic processes lead to averaging of spacial positions resulting in an effective higher symmetry which reduces the width of the sideband pattern, as nicely seen in Figure 3b.

An inspection of the temperature-dependent lineshape changes in the ^{13}C NMR spectrum (Fig. 1) suggests at first sight a simple two-site exchange process for the methylene carbons, where the doublet observed at 190 K broadens and shows coalescence at ca. 224 K. A closer look at the temperature-induced spectral changes indicates, however, that a simple two-site exchange process is not adequate to explain the experimental observations. As Fig. 1 demonstrates, after coalescence around 224 K, where linenarrowing is expected, further broadening occurs for the CH_2 signal which is nearly lost in the noise around 270 K. It is only at elevated temperatures (> 314 K) that a singlet with reduced linewidth can be observed. We ascribe this phenomenon to *dipolar broadening* [12] which results from an increased transverse relaxation of the respective nuclei in a situation where the power of the proton decoupler field B_2 matches the exchange rate between non-equivalent positions. At the point of largest linewidth, the condition

$$\gamma B_2 = 1/\tau_c \tag{1}$$

holds and the exchange rate $k = 1/\tau_c$ can be determined if the power of the decoupling field is known. It is interesting to note that the failure to observe the CH_2 resonance in the earlier investigations [16], which were performed at lower field strength, can now be ascribed to this dipolar broadening effect.

In order to characterize the dynamic process associated with the described changes in the ^{13}C NMR spectrum more quantitatively, a lineshape simulation based on a simple two-site exchange process [24] was performed for spectra measured in the range between 190 K and 224 K. As can be seen from a comparison of calculated and observed spectra given in Fig. 4, the effect of dipolar broadening already contributes to the linewidths at 214 and 224 K, and these data were thus

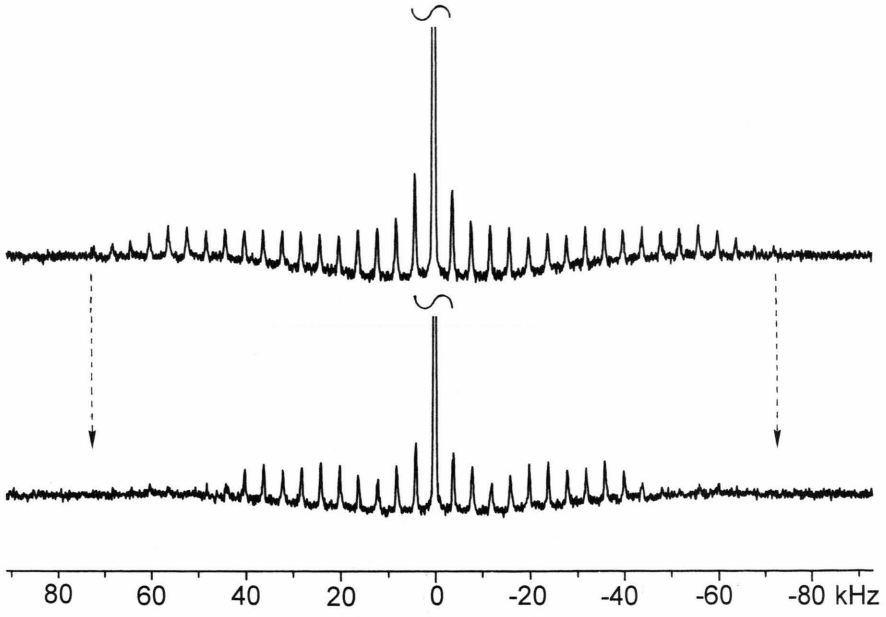

Fig. 3. 116.64 MHz ^{7}Li MAS NMR spectrum of **1** at 297 K (above, a) and 340 K (below, b); spinning speed 4 kHz.

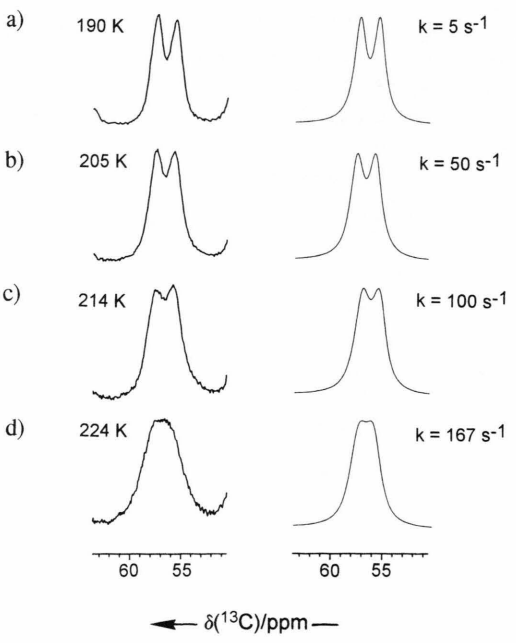

Fig. 4. ^{13}C NMR resonances of the methylene carbons of **1** at different temperatures: experimental (left) and calculated (right); for exp. details see exp. part.

not included in the analysis. From the two calculated rate constants of 5 and 50 s^{-1} (cf. exp. part), observed in a temperature region where the additional broadening effect due to proton decoupling should be negligible, one derives Eyring activation parameters $\Delta H^{\neq}$ of 48.8 kJ mol^{-1} and $\Delta S^{\neq}$ of 28 J mol^{-1} K^{-1}. On including the information from the point of largest dipolar broadening at 270 K, an additional rate constant of 71.400 s^{-1} is obtained on the basis of (1) (cf. exp. part), and the energy barrier derived from the three measurements is again 48.8 kJ mol^{-1}, and $\Delta S^{\neq} = 28$ J mol^{-1} K^{-1}, in excellent agreement with the data from the lineshape calculations alone (Figure 5).

For a quantitative analysis of the ^{15}N spectra, a lineshape calculation was not successful. This is not surprising, considering the small chemical shift difference, $\delta\nu$, the large natural linewidth, and the limited temperature range for these spectral changes. However, at coalescence ($T_c = 326$ K) a free energy of activation $\Delta G^{\neq}$ (326) of 68 kJ mol^{-1} can be derived by the well-known relation [25]

$$\Delta G^{\neq} = R\,T_c[22.96 + \ln(T_c/\delta\nu)]. \qquad (2)$$

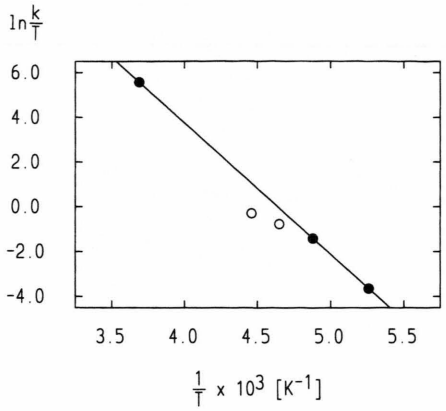

Fig. 5. Eyring plot of the kinetic data for the low-temperature dynamic process observed for **1**; o data obtained at 214 and 224 K and not included in the analysis.

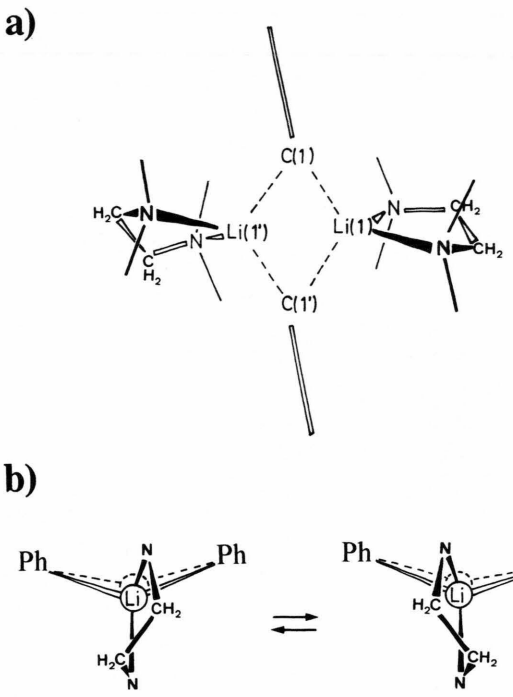

Fig. 6. Stereochemistry of **1** (schematically) as determined by X-ray analysis [6].

According to these observations, two independent dynamic processes are detected for **1**, which are characterized by energy barriers $\Delta G^{\neq}$ (326) of 40 and 68 kJ mol^{-1}, respectively. In order to assign these barriers to specific dynamic processes, we have to consult the X-ray data [6]. The most important stereochemical aspects relevant for our discussion are summarized in Figure 6a. The non-equivalence of the two methylene carbons is a result of the twisted conformation of the five-membered ring composed of the metal atoms and the TMEDA ligands, and the skew arrangement found for the phenyl rings. In discussing the X-ray results, it was already noted [6] that the ethylene bridge is heavily twisted, and the large temperature factors of the atoms involved pointed to a strong thermal mobility in this part of the complex. It is, therefore, justified to assign the dynamic process with the lower energy barrier to the ring inversion of the five-membered ligand ring (Figure 6b). However, considering the non-equivalence of the two methylene carbons, which should remain due to the non-planarity of the central four-membered ring composed of the two lithium atoms and the two *ipso*-carbons of the aromatic units [C(1)–Li(1)–C(1′)–Li(1′), Fig. 6], one must conclude that this effect is most probably less pronounced, or, what is more likely, masked by the dipolar line-broadening observed for these signals.

As Fig. 6b demonstrates, the non-equivalence of the nitrogens results from the non-planarity of the central four-membered ring. The ring inversion process discussed above for the Li^+-TMEDA moiety clearly does not affect the chemical environment of the nitrogen atoms, and their equivalence above 326 K must be a consequence of either the inversion of the central four-membered C(1)–Li(1)–C(1′)–Li(1′) ring or a complete rotation of the TMEDA ligand around an axis which passes through the centre of the ethylene CC bond and the lithium atom. The higher energy barrier of 68 kJ mol^{-1} is then assigned to one or the other of these processes. A concerted action of both movements is not possible since this would bring the nitrogens in equivalent positions and leave the ^{15}N spectrum unchanged.

As is clearly seen from the ^{13}C NMR spectra (Fig. 1), increasing temperature (> 300 K) also leads to reversible lineshape changes for the remaining carbon signals, which indicates an averaging of spacial positions due to increased *intra*-aggregate mobility also for the other atoms. In particular the environment of the methyl carbons changes, and this leads to a CH_3 singlet at elevated temperatures, a process which parallels the changes observed in the ^{15}N NMR spectrum. It is not clear, however, if a true coalescence process is involved or if the changes are due to a temperature dependence of the ^{13}C chemical shifts. In

any case, the chemical shift difference involved here is ca. twice that in the ^{15}N spectrum. An increased coalescence temperature is thus to be expected because the same dynamic process which averages the ^{15}N environment should average the environment of the CH_3 groups.

2. *Lithiumcyclopentadienide, [Li(tmeda)]C_5H_5 (2)*

Not unexpectedly, compound **2** shows a much simpler behaviour than the complex **1**. At RT the ^{13}C CP/MAS NMR spectrum yields only two lines (CH and CH_3 carbons), with the resonance of the methylene carbons missing (Figure 7a). Only at elevated temperatures (343 K) is this resonance seen as a broadened signal (Fig. 7b and (Table 1), again indicating a dynamic process in the five-membered ring formed by the central metal and the TMEDA ligand. In the same direction points the observation that, in contrast to the situation met for **1**, only one CH_3 signal is found for **2**. The large temperature factors reported in the X-ray study of the tris-trimethylsilyl derivative of **2** [7] support this interpretation. Again, as in the case of **1**, the ^{13}C chemical shifts do not differ significantly from the data determined in solution (Table 1). Only one ^{15}N signal is found for **2** (Table 2), and the ^{7}Li at -5.7 ppm (rel. to LiBr) shows the ring current effect as in solution, where -8.7 ppm was found [26]. It is interesting to note that the solid state value agrees very well with the Li shielding calculated by the IGLO method (-6.9 ppm) [27].

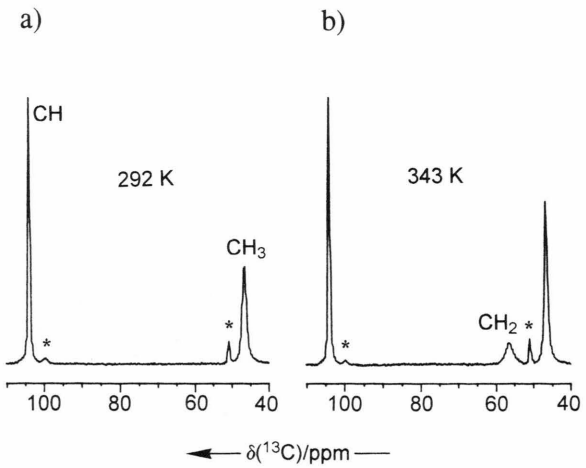

Fig. 7. ^{13}C CP/MAS NMR spectra of [Li(tmeda)]C_5H_5 (**2**) at different temperatures.

Table 3. Shielding tensor elements for **2** and ferrocene as calculated by the Herzfeld-Berger method [29] (**A**) and the analysis of moments [30] (**B**).

	2[a]		ferrocene[a]		ferrocene[b]
	A	**B**	**A**	**B**	
σ_{iso}/ppm	−103.9	−103.9	−69.5	−69.5	69
$\sigma_{11}-\sigma_{iso}$/ppm	−45.8	−45.5	−31.2	−29.7	−25
$\sigma_{22}-\sigma_{iso}$/ppm	−23.9	−32.3	−19.4	−20.6	−25
$\sigma_{33}-\sigma_{iso}$/ppm	69.6	77.7	50.6	50.3	51
η	0.31	0.17	0.23	0.18	0

[a] This work;
[b] [28].

It is reasonable to expect axial symmetry for **2** on the NMR time scale at RT, in analogy to observations made for ferrocene [28]. In line with the fast rotation of the five-membered ring formed by the TMEDA ligand and the metal around the effective C_5 symmetry axis of the compound is the presence of only one ^{13}C signal for the carbocyclic ring. In addition, a NQS experiment again allows detection of the resonances of all protonated carbons (CH, CH_2, CH_3) even with a dephasing period of 70 μs. No attempts were made to investigate low-temperature spectra of **2**.

From an analysis of the sideband pattern shown in Fig. 8, based on the Herzfeld-Berger method [29] and the method of moments [30], it was possible to calculate the chemical shift tensor components, σ_{ii}, and the asymmetry parameter, η, for the methine carbons of the five-membered cyclopentadienyl ring. The results are shown in Table 3, together with those of a sample calculation for ferrocene. In agreement with our expectations, the asymmetry parameter η is close to zero, the deviation from the theoretical value zero coming from inherent inaccuracies of the sideband analysis.

A further documentation of the effective axial symmetry which governs the NMR spectra of **2** at RT comes from the static ^{7}Li powder spectrum (Fig. 9), which shows the typical satellite pattern characteristic for first order quadrupolar interaction of a nucleus with spin quantum number $I = 3/2$ with zero asymmetry parameter [23b, 31]. From the satellite splitting a quadrupolar coupling constant of ca. 150 kHz can be derived, in good agreement with results for the TMEDA complex of trimethylsilylcyclopentadienyllithium (**4**) [32], where an effective axial symmetry of the electric field gradient tensor at the metal was detected.

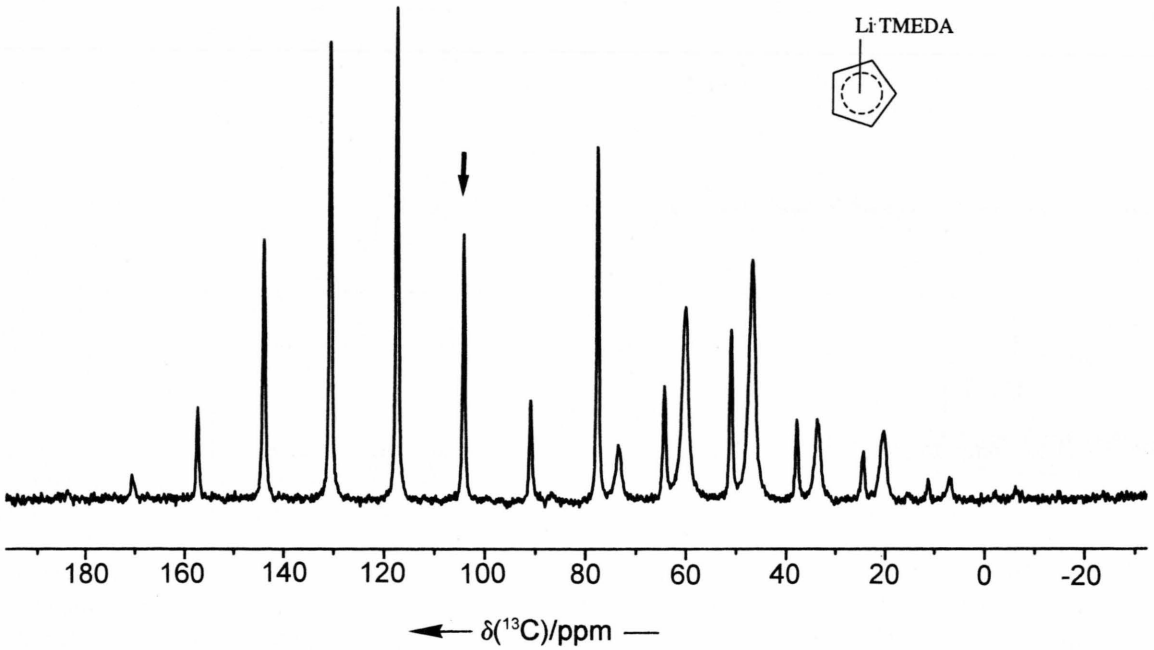

Fig. 8. Sideband pattern in the ^{13}C CP/MAS NMR spectrum of **2** at RT.

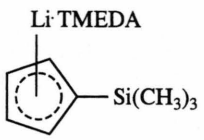

4

3. Dilithiumnaphthalenediide, trans-[Li(tmeda)]$_2C_{10}H_8$ (3)

Finally we discuss results obtained for the TMEDA complex of dilithiumnaphthalenediide (**3**), a compound of considerable interest because of its application in various metallation reactions, most notably in anionic polymerisations [33]. NMR data for **3** in solution are available [21], and the data found now for the solid are again not significantly different (Table 1). The carbocyclic ligand of **3** constitutes a paramagnetic 12 π dianion [21], and the X-ray structure [5] shows C_i symmetry for the complex where the two lithium atoms are situated above and below the two six-membered rings of the naphthalene nucleus (**3**). The coordinated TMEDA ligands are inclined to the axis which connects carbons 1 and 4 as well as 5 and 8 by an angle of ca. 70%, as is shown schematically in diagram 5.

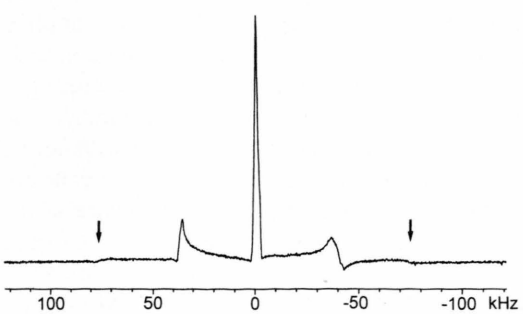

Fig. 9. Static ^7Li MAS NMR spectrum of **2** at RT.

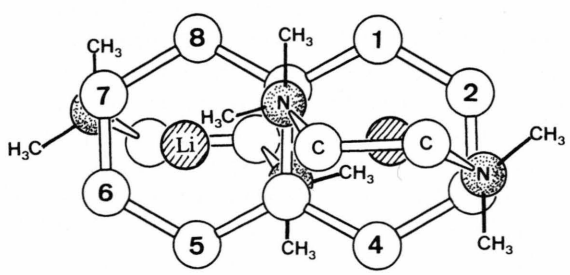

5

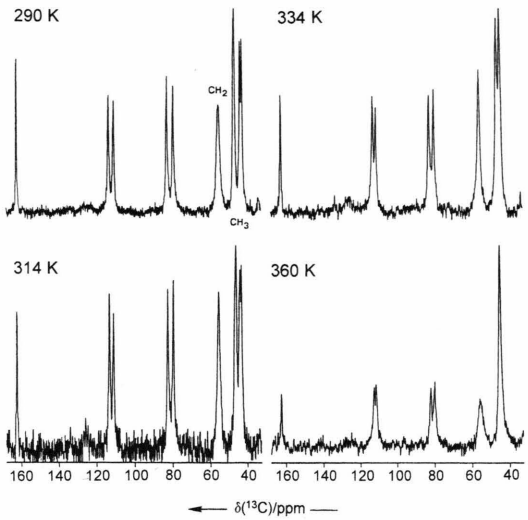

Fig. 10. ^{13}C CP/MAS spectra of *trans*-[Li(tmeda)]$_2C_{10}H_8$ (**3**) at different temperatures.

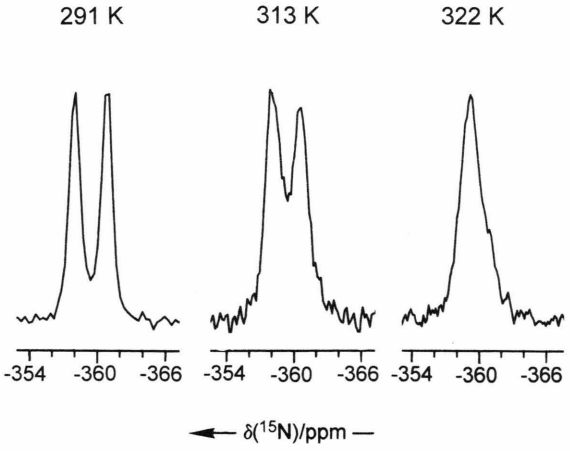

Fig. 11. Temperature dependence of the ^{15}N CP/MAS NMR spectrum of **3**.

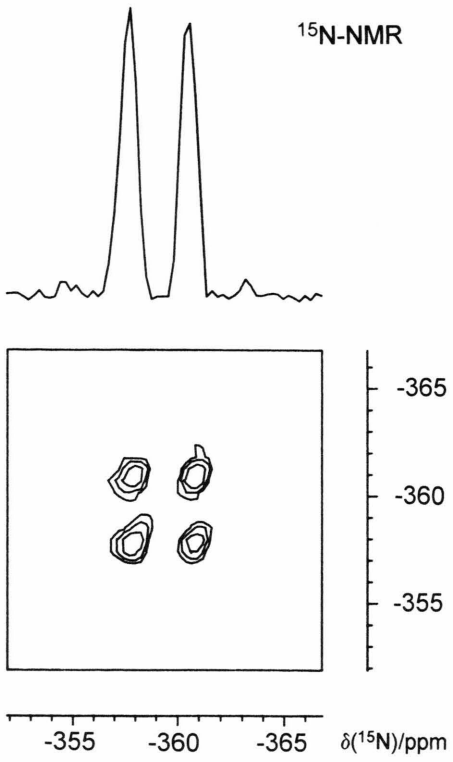

Fig. 12. Two-dimensional natural abundance ^{15}N EXSY spectrum of **3** at 292 K; spinning rate 2.5 kHz.

The ^{13}C CP/MAS solid state NMR spectrum of **3** (Fig. 10) is in line with the structure of C_i symmetry and shows the expected five resonances for the carbocyclic ringsystem, one somewhat broadened resonance for the CH_2 carbons and four signals for the CH_3 groups (Table 1). The skewed arrangement of the two TMEDA ligands is also documented by the ^{15}N CP/MAS NMR spectrum, which shows a RT two resonances separated by 2.9 ppm (Table 2).

Except for nearly linear temperature-induced resonance shifts, the ^{13}C NMR spectrum is not much affected by temperature variations between 290 and 360 K. Specifically no coalescence phenomena are observed. In contrast, the ^{15}N resonance broadens at elevated temperatures and finally coalesces into a single line (Figure 11). Chemical exchange between the two nitrogen sites is most clearly seen from the two-dimensional exchange spectrum shown in Fig. 12, which was measured with a modified $90° - t_1 - 90° - t_M - 90°$, FID ($t_2$) pulse experiment, the first 90° pulse being replaced by the CP sequence [14]. At the coalescence temperature (317 K) we derive, on the basis of (2), a barrier $\Delta G^{\neq}$ of 64 kJ mol^{-1} for the dynamic process which leads to the equivalence of the two nitrogen atoms. We assign this process to a 180° rotation of the TMEDA ligands (**A** $\rightleftharpoons$ **B** $\rightleftharpoons$ **C**). A simple oscillation of the type **D** $\rightleftharpoons$ **E** does not explain the experimental observations because in this case coalescence of the ^{13}C resonances for C-1 and C-4 as well as for C-2 and C-3 should be observed. Furthermore, an oscillation demands a concerted movement of both TMEDA ligands, which is not required for the 180° rotation.

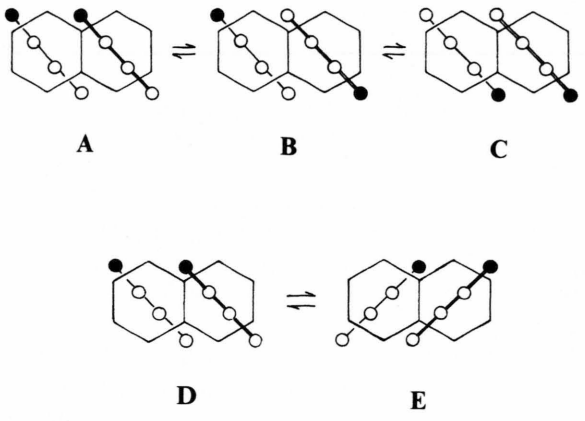

Looking again at diagram **5**, for a 180° rotation of the Li^+-TMEDA unit accompanied by ring inversion one also expects lineshape changes for the CH_2 and CH_3 resonances. There is indeed a specific broadening effect for the CH_2 resonance, where the linewidth changes from 171 to 117 Hz between 290 and 334 K. The CH_3 signals, on the other hand, first merge to a doublet (334 K) and later into a singlet (360 K). There is no clear indication of a coalescence process because the linewidth is apparently not much affected and part of the signal merging is the result of the temperature-dependent chemical shifts. Thus, the information from the ^{13}C spectrum alone does not allow to draw any conclusions about the *intra*-aggregate dynamics of **3**.

Conclusions

In comparing our results with those of related investigations performed on other TMEDA complexes in solution, we find that similar barriers have been reported for processes that lead to coalescence phenomena in the ^1H and ^{13}C NMR spectra [3, 34], but an unambiguous assignment of these spectral changes to either ring inversion or rotation of the TMEDA ligands was not achieved. In addition, a third mechanism which involves breaking of a nitrogen-lithium bond and recombination was discussed [4]. On the other hand, theoretical calculations on the MNDO and ab initio level [34] led to the conclusion that a composite of ring inversion and rotation might be responsible for the observed NMR lineshape changes and that both processes have similar activation barriers. Our results now demonstrate for the solid that ring inversion and full rotation are characterized by two distinct energy barriers, where the free activation enthalpy for the second process is considerably larger than that for the first one. In solution, this difference might indeed be smaller because, due to packing forces, ring rotation in the solid is probably more hindered than in solution. The calculated barrier of ca. 30 kJ mol^{-1} [34] for the ring inversion process in the gas phase compares favourably with our results for solid **1**. In addition, since the barrier found for Li^+-TMEDA rotation in **3** is close to that for the second dynamic process in **1**, the higher energy process operating in **1** is most likely also a Li^+-TMEDA rotation.

Acknowledgements

We are indebted to Prof. R. K. Harris, Durham, for helpful discussions, to the Volkswagen-Stiftung for a spectrometer grant, and to the Fonds der Chemischen Industrie, Frankfurt, for financial support. W. B. thanks the Graduiertenkolleg "Chemical Reactivity and Molecular Order" for a postdoctoral fellowship. Y. O. gratefully acknowledges a grant from the Alexander-von-Humboldt foundation.

Experimental Part

Compounds and Sample Preparation

The synthesis of **1**–**3** followed the literature procedures: **1** [6]; **2** [7], and **3** [5]. The samples used for the NMR experiments were purified by recrystallization under argon and did not show any NMR absorptions due to impurities. For the NMR measurements, 4 mm (^{13}C, ^7Li) or 7 mm (^{15}N) o.d. ZrO_2 rotors were filled under argon with 100–150 mg or 250–300 mg, respectively, of the compounds and tightly locked with Kel-F caps. This proved to be sufficient for keeping the rotors air-tight during the measurements. Even after storage for several months no decomposition of organometallic material was detected by NMR-spectroscopy.

NMR Spectra

NMR spectra were measured with a Bruker MSL 300 spectrometer, operating at 75.47 MHz for ^{13}C, 30.42 MHz for ^{15}N, and 116.64 MHz for ^7Li, and equipped with a variable temperature unit and ^1H decoupling channel. High-power CW proton decoupling was applied through all acquisitions. For ^{13}C

and ^{15}N CP/MAS measurements, typical contact times were 1–2 ms, with a ^{1}H 90° pulse width of 3–6 μs. For the ^{7}Li MAS spectra, the 90° pulse width was 3.6 μs. Spectra of static samples were recorded with the Quadecho sequence [35] with a delay of 150 μs. Chemical shifts were referenced externally against adamantane ($^{13}C(CH_2)$ δ 38.4 ppm rel. to TMS), NH_4Cl (^{15}N, δ −341.3 ppm rel. to nitromethane), and LiBr (^{7}Li, $\delta = 0$). For the ^{15}N 2D EXSY spectrum, measured at 295 K, the following spectral parameters were used: spectral width 2 kHz, contact time 2 ms, mixing time 1 s, 128 experiments in t_1 (200 scans each), t_1 increment 250 μs, recycle delay 7 s, phase-sensitive detection by the TPPI method [36], total spectrometer time 54 hrs. The final data matrix was $512(t_2) \times 256(t_1)$, no window functions were applied. The calculations of the tensor components for **2** were performed with the Bruker MASNMR software.

For the lineshape calculations a program based on the Gutowsky-Holm theory [11, 24] was used. The relevant parameters for the ^{13}C CH_2 signal of **1** were $\delta\nu = 142$ Hz and 100 Hz natural linewidth. The rate constants calculated are given in Figure 1. The decoupler field strength was calculated from the pulse width of the 90° ^{1}H pulse (3.5 μs) [37]. For the ^{15}N signal of **1**, $\delta\nu$ was 44 Hz and the coalescence temperature 326 K. In the case of the ^{15}N signal of **3** we used $\delta\nu = 90$ Hz at $T_c = 317$ K. The temperature readings of the temperature control unit were corrected on the basis of a calibration using the methanol and ethylene glycol shift thermometers [38].

[1] Reviews: a) M. Schlosser, Polare Organometalle, Springer Verlag, **1973;** b) J. L. Wardell, in Comprehensive Organometallic Chemistry, Vol. 1, p. 43 ff., G. Wilkinson, F. G. A. Stone, and E. W. Abel, Eds., Pergamon Press **1982;** b) K. Gregory, P. v. R. Schleyer, and R. Snaith, Adv. Inorg. Chem. **37,** 47 (1991); c) A. Maercker and M. Theis, Top. Curr. Chem. **138,** 1 (1987); d) E. Weiss, Angew. Chem. **105,** 1565 (1993); Angew. Chem. Int. Ed. Engl. **32,** 1501 (1993).

[2] Reviews: a) T. L. Brown, Acc. Chem. Res. **1,** 23 (1968); b) W. Bauer and P. v. R. Schleyer, in "Advances in Carbanion Chemistry", ed. V. Snieckus, Jai Press, Greenwich (Connecticut), 1992, p. 89.

[3] See for example G. Fraenkel, A. Chow, and W. R. Winchester, J. Amer. Chem. Soc. **112,** 1382 (1990).

[4] K. Gregory, M. Bremer, W. Bauer, P. v. R. Schleyer, N. P. Lorenzen, J. Kopf, and E. Weiss, Organometallics **9,** 1485 (1990).

[5] J. J. Brooks, W. Rhine, and G. D. Stucky, J. Amer. Chem. Soc. **94,** 7346 (1972).

[6] D. Thoennes and E. Weiss, Chem. Ber. **111,** 3157 (1978).

[7] P. Jutzi, E. Schlüter, S. Pohl, and W. Saak, Chem. Ber. **118,** 1959 (1985).

[8] M. F. Lappert, A. Singh, L. M. Engelhardt, and A. H. White, J. Organomet. Chem. **262,** 271 (1984).

[9] a) W. N. Setzer and P. v. R. Schleyer, Adv. Organomet. Chem. **24,** 353 (1985); b) J. J. Brooks and G. D. Stucky, J. Amer. Chem. Soc. **94,** 7333 (1972).

[10] J. R. Lyerla, C. S. Yannoni, and C. A. Fyfe, Acc. Chem. Res. **15,** 208 (1982).

[11] J. Sandström, Dynamic NMR Spectroscopy, Academic Press, London 1982.

[12] W. P. Rothwell and J. S. Waugh, J. Chem. Phys. **74,** 2721 (1981).

[13] J. Jeener, B. H. Meier, P. Bachmann, and R. R. Ernst, J. Chem. Phys. **71,** 4546 (1979); for a review see C. L. Perrin and T. J. Dwyer, Chem. Rev. **90,** 935 (1990).

[14] J. M. Twyman and C. M. Dobson, Magn. Reson. Chem. **28,** 163 (1990).

[15] F. G. Riddell, S. Arumugam, K. D. M. Harris, M. Rogerson, and J. H. Strange, J. Amer. Chem. Soc. **115,** 1881 (1993).

[16] D. Johnels and U. Edlund, J. Organomet. Chem. **393,** C35 (1990).

[17] D. Johnels, J. Organomet. Chem. **445,** 1 (1993).

[18] O. Eppers and H. Günther, Helv. Chim. Acta **75,** 2553 (1992); O. Eppers, Ph.D. thesis, University of Siegen, 1992.

[19] H.-O. Kalinowski, S. Berger, and S. Braun, "^{13}C-NMR-Spektroskopie", Thieme, Stuttgart 1984, p. 377.

[20] P. Jutzi, W. Leffers, S. Pohl, and W. Saak, Chem. Ber. **122,** 1449 (1989).

[21] R. Benken and H. Günther, Helv. Chim. Acta **71,** 694 (1988).

[22] S. J. Opella and D. M. H. Frey, J. Amer. Chem. Soc. **101,** 5854 (1979).

[23] See a) J. E. Espidel, R. K. Harris, and K. Wade, Magn. Reson. Chem. **32** (1994); b) R. K. Harris and C. A. Fyfe, in Multinuclear Magnetic Resonance in Liquids and Solids – Chemical Applications, R. K. Harris and P. Granger, eds., NATO ASI Ser. C322, Kluwer, Dordrecht (1990), p. 269, 311.

[24] H. S. Gutowsky and C. H. Holm, J. Chem. Phys. **25,** 1228 (1956).

[25] H. Günther, "NMR-Spektroskopie", 3. Aufl., G. Thieme, Stuttgart 1992, S. 310.

[26] R. H. Cox and H. W. Terry, Jr., J. Magn. Reson. **14,** 317 (1974).

[27] L. A. Paquette, W. Bauer, M. R. Sivik, M. Bühl, M. Feigel, and P. v. R. Schleyer, J. Amer. Chem. Soc. **112,** 8776 (1990).

[28] D. E. Wemmer and A. Pines, J. Amer. Chem. Soc. **103,** 34 (1981).

[29] J. Herzfeld and A. E. Berger, J. Chem. Phys. **73,** 6021 (1980).

[30] M. M. Maricq and J. S. Waugh, J. Chem. Phys. **73,** 6026 (1982).

[31] J. F. Hon and P. J. Bray, Phys. Rev. **110,** 624 (1958).

[32] T. Pietraß and P. K. Burkert, Z. Naturforsch. **48b,** 1555 (1993).

[33] W. Schlenk and E. Bergmann, Liebigs Ann. Chem. **463,** 91 (1928).

[34] G. Boche, G. Fraenkel, J. Cabral, K. Harms, N. J. R. van Eikema Hommes, J. Lohrenz, M. Marsch, and P. v. R. Schleyer, J. Amer. Chem. Soc. **114,** 1562 (1992).

[35] J. H. Davis, K. R. Jeffrey, M. Bloom, M. I. Valic, and T. P. Higgs, Chem. Phys. Lett. **42,** 390 (1976).

[36] D. Marion and K. Wüthrich, Biochem. Biophys. Res. Commun. **113,** 967 (1983).

[37] A. Bax, J. Magn. Reson. **52,** 76 (1983).

[38] M. Ebener, Ph.D. thesis, University of Siegen 1994.